J Neurophysiol 101: 54–66, 2009.
First published November 12, 2008; doi:10.1152/jn.91020.2008.

Random Stimulation of Spider Mechanosensory Neurons Reveals Long-Lasting Excitation by GABA and Muscimol

Keram Pfeiffer, Izabela Panek, Ulli Höger, Andrew S. French, and Päivi H. Torkkeli
Department of Physiology and Biophysics, Dalhousie University, Halifax, Nova Scotia, Canada

Submitted 12 September 2008; accepted in final form 6 November 2008

Pfeiffer K, Panek I, Höger U, French AS, Torkkeli PH. Random stimulation of spider mechanosensory neurons reveals long-lasting excitation by GABA and muscimol. *J Neurophysiol* 101: 54–66, 2009. First published November 12, 2008; doi:10.1152/jn.91020.2008. γ-Aminobutyric acid type A ($GABA_A$) receptor activation inhibits many primary afferent neurons by depolarization and increased membrane conductance. Deterministic (step and sinusoidal) functions are commonly used as stimuli to test such inhibition. We found that when the VS-3 mechanosensory neurons innervating the spider lyriform slit-sense organ were stimulated by randomly varying white-noise mechanical or electrical signals, their responses to $GABA_A$ receptor agonists were more complex than the inhibition observed during deterministic stimulation. Instead, there was rapid excitation, then brief inhibition, followed by long-lasting excitation. During the final excitatory phase, VS-3 neuron sensitivity to high-frequency signals increased selectively and their linear information capacity also increased. Using experimental and simulation approaches we found that the excitatory effect could also be achieved by depolarizing the neurons without GABA application and that excitation could override the inhibitory effect produced by increased membrane conductance (shunting). When the VS-3 neurons were exposed to bumetanide, an antagonist of the Cl^- transporter NKCC1, the GABA-induced depolarization decreased without any change in firing rate, suggesting that the effects of GABA can be maintained for a long time without additional Cl^- influx. Our results show that the VS-3 neuron's response to GABA depends profoundly on the type of signals the neuron is conveying while the transmitter binds to its receptors.

INTRODUCTION

Activation of γ-aminobutyric acid type A ($GABA_A$) receptors opens ion channels permeable to Cl^- and HCO_3^-. Depending on the equilibrium potentials of these anions, currents through $GABA_A$ channels either hyperpolarize or depolarize neuronal membrane (Marty and Llano 2005). Hyperpolarization is the typical response in mature central neurons and leads to inhibition. In contrast, depolarization has diverse consequences in different cells and developmental states. In many vertebrate neonatal and some mature central neurons, as well as in anterior pituitary cells, GABA-mediated depolarization leads to excitation (Ben-Ari 2002; Marty and Llano 2005; Zemkova et al. 2008), whereas in mammalian and invertebrate primary afferent mechanosensory neurons depolarization and an increase in membrane conductance (shunting) cause presynaptic inhibition (Clarac and Cattaert 1996; Nusbaum et al. 1997; Rudomin and Schmidt 1999).

GABA-induced depolarization and shunting also occur in the peripherally located parts of mechanosensory neurons innervating the VS-3 lyriform slit-sense organ in the patella of the spider *Cupiennius salei*. The VS-3 organ consists of seven to eight cuticular slits, each innervated by a pair of bipolar mechanosensory neurons (Barth and Libera 1970) with somata of 20–100 μm in diameter. The 50- to 300-μm-long sensory dendrites are attached to the slits via a specialized cuticular structure (French et al. 2002). Peripherally located parts of these neurons are surrounded by thin efferent fibers (Fabian-Fine et al. 1999) that have been shown to contain GABA, glutamate, and octopamine (Fabian-Fine et al. 1999, 2002; Widmer et al. 2005).

When VS-3 neurons were stimulated by step stimuli, application of $GABA_A$ receptor agonists (muscimol or GABA) inhibited firing (Panek et al. 2002). When action potential (AP) responses to mechanical stimuli were recorded extracellularly at different locations, the inhibitory response could be detected only at the axonal region, suggesting that the $GABA_A$ receptors may be located only at the axons (Gingl et al. 2004). In nature, the slits are believed to respond to strains and vibrations that occur in the spider's environment or are elicited by body movements (Barth 2001; Seyfarth 1985). Natural stimuli include movements caused by wind, by predators and prey, and the movements of potential mates during courtship behavior. These types of signals contain a variety of frequency components that probably vary strongly with the behavioral situation and are quite different from the deterministic stimuli previously used to assess efferent modulation.

To learn how $GABA_A$ receptor activation influences the dynamic behavior of VS-3 neurons we tested the responses of these neurons to a broad band of stimulus frequencies while GABA or muscimol was applied. Previous investigations showed that the distal dendrites of VS-3 neurons generate APs and that the inhibitory response to $GABA_A$ agonists occurs only in the axonal region (Gingl and French 2003; Gingl et al. 2004). To learn whether the changes in the dynamic behaviors of dendritic and axosomatic regions are different when the $GABA_A$ receptor agonist muscimol is applied, we performed two series of experiments using either mechanical stimuli to generate dendritic APs or electrical stimuli to generate axosomatic APs. In both types of experiments muscimol caused a triphasic response consisting of fast excitation, followed by inhibition and a long-lasting excitation. To investigate potential mechanisms that may produce the final excitatory response we used both experimental and previously established modeling approaches (Torkkeli and French 2002). To learn whether the excitatory effects of GABA in VS-3 neurons are controlled by

Address for reprint requests and other correspondence: P. H. Torkkeli. Department of Physiology and Biophysics, Dalhousie University, Halifax, Nova Scotia, Canada B3H 1X5 (E-mail: Paivi.Torkkeli@dal.ca).

The costs of publication of this article were defrayed in part by the payment of page charges. The article must therefore be hereby marked "*advertisement*" in accordance with 18 U.S.C. Section 1734 solely to indicate this fact.

specific Cl^- transporters, as has been shown in other invertebrate and vertebrate preparations (Cheung et al. 2006; Choi et al. 2008; Dzhala et al. 2005), we tested the effects of two Cl^- transporter antagonists, bumetanide and furosemide, on the excitatory GABA response.

METHODS

Experimental animals

Tropical wandering spiders (*Cupiennius salei*) (Fig. 1*A*) were maintained in a laboratory colony at room temperature (22 ± 2°C) and a 13:11-h light:dark cycle. For all experiments, legs from adult spiders were autotomized following a protocol approved by the Dalhousie University Committee on Laboratory Animals. Two different experimental preparations were used: *1*) Cuticular preparation where a piece of cuticle, containing the intact VS-3 slit-sense organ was cut from the leg and waxed to a Plexiglas holder that permitted access to both the outer and inner surfaces of the organ (Fig. 1*B*) (Juusola et al. 1994; Seyfarth and French 1994). *2*) Hypodermis preparation, for which the VS-3 organ was removed from the cuticle, mounted on a 1-mg/ml poly-L-lysine-coated coverslip, and used in experiments where only electrical stimulation was applied. A detailed description of this preparation was previously published (Sekizawa et al. 1999).

Recording and stimulation

Neurons were visualized using an upright compound microscope Axioskop 2 FS Plus with Epiplan ×10 or Achroplan ×40 water-immersion objective (Zeiss, Oberkochen, Germany), mounted on a gas-driven vibration isolation table inside a Faraday cage (Technical Manufacturing, Peabody, MA). Sharp borosilicate glass microelectrodes (OD, 1 mm; ID, 0.5 mm; Hilgenberg, Malsfeld, Germany) were pulled using a P-2000 horizontal laser puller (Sutter Instrument, Novato, CA). Electrodes were filled with 3 M KCl and they had resistances between 40 and 100 MΩ in solution. Recordings were made in discontinuous single-electrode current-clamp– or voltage-clamp–controlled current-clamp (VCcCC) mode (Sutor et al. 2003) using SEC-10L or SEC-10LX amplifier with a VCcCC addendum (npi elektronic, Tamm, Germany). Switching frequencies between18 and 20 kHz and a duty cycle 1/4 or 1/8 (current passing/voltage recording) were used. The voltage was low-pass filtered at 33.3 kHz and the current signal was filtered at 3.3 kHz by the amplifier. Neuronal somata were impaled with the microelectrodes using a PatchStar (Scientifica, Uckfield, UK) or Burleigh TS-5000 (Burleigh Instruments, Victor, NY) micromanipulator.

Neurons were stimulated either electrically via the recording electrode or mechanically using a piezoelectric stimulator (P-841.20 actuator, and P-862.00 LVPZ controller, Physik Instrumente, Karlsruhe, Germany) that pushed a glass probe against the slits from below (Fig. 1*B*). Deflection of 0.3 μm was adequate to evoke electrical activity in the sensory neurons. The mechanical stimulator response (in feedback loop-controlled mode) was low-pass, falling by −6 dB at 70 Hz, which limited its performance at higher frequencies.

IBM-compatible personal computers were used for all data recording and stimulation using custom-written software. Current, voltage, and mechanical signals were provided by the computer via a 12-bit D/A converter and recorded via a 16-bit A/D converter (National Instruments, Austin, TX). The stimulus consisted of pseudorandom Gaussian white noise generated by the computer via a 33-bit binary-sequence algorithm. For the electrical stimulation this signal was low-pass filtered at 300 Hz, using a custom-built nine-pole active filter. Action potentials were detected by a threshold-detection algorithm (French et al. 2001) and stored as time of occurrence. Examples of experiments with mechanical and electrical stimuli with resulting AP trains are shown in Fig. 1, *C* and *D*. The AP signals were digitally filtered by convolution with a sin $(x)/x$ function and resampled at 1 kHz, to band-limit the frequency range to 0–500 Hz (French and Holden 1971). The resulting signal was used as output signal in the subsequent frequency response analysis. The probe position served as an input signal when mechanical stimulation was applied. The input signal for recordings with electrical stimulation was obtained by removing APs from the intracellular recording through deletion of 2 ms of samples around each AP and filling the resultant gap by linear

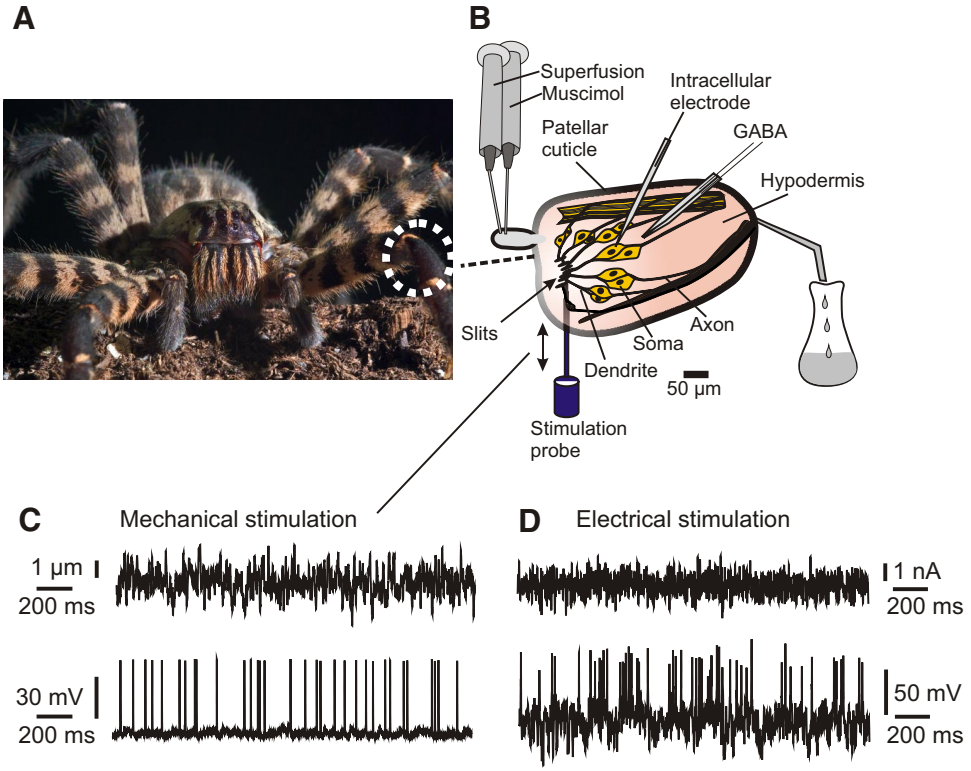

FIG. 1. Experimental arrangement. *A*: portrait of a female wandering spider (*Cupiennius salei*). Dashed circle shows anterior part of the patella, where the VS-3 lyriform organ is located. *B*: a piece of cuticle was cut from the patella and mounted to allow mechanical stimulation from below and intracellular recording from above. The preparation was superfused continuously with spider saline and in the "cuticular preparation" muscimol was injected into the superfusion solution. For the "hypodermis preparation" VS-3 organ was detached from the cuticle and placed on a recording chamber where a similar superfusion system was used for saline and antagonist application, but γ-aminobutyric acid (GABA) was applied using an iontophoretic system. Location of iontophoretic double-barrel electrode is also shown. Pseudorandom noise stimuli were applied either via the stimulation probe or as current injections through the recording electrode. *C* and *D* show portions of the raw data with mechanical (*C*) and electrical (*D*) pseudorandom white noise stimuli (above) and the resulting action potentials (below).

interpolation. Input and output signals were digitally resampled at 1 kHz and then transferred to the frequency domain using the fast Fourier transform (Cooley and Tukey 1965) in segments of 512 or 1,024 input–output data pairs. Frequency response functions were plotted as Bode plots (phase and log gain vs. log frequency) and fitted by the power-law relationship

$$G = Af^k \quad (1)$$

$$P(f) = k\ 90° - \Delta t\ f\ 360° \quad (2)$$

where f is frequency; A is a constant describing overall sensitivity (gain at 1 Hz); k is the fractional exponent, corresponding to adaptation; $P(f)$ is the phase lag as a function of frequency; and Δt is the time delay. Fitting was performed on the complete frequency response function in complex exponential format to obtain a minimum squared error between the experimental and fitted values.

Coherence functions, $\gamma^2(f)$ (Bendat and Piersol 1980) between the input and output were calculated and plotted against log frequency. Linear information capacity (R) was calculated from the coherence functions using the Shannon formula (Shannon and Weaver 1949)

$$R = \int \log_2 \left[\frac{1}{1 - \gamma^2(f)} \right] df \quad (3)$$

Statistical analysis

Statistical analysis was performed using Prophet 6.0 software (AbTech, Charlottesville, VA). For the paired data sets where values were normally distributed a paired t-test was used to determine the difference between means. When the distribution assumptions for t-test were not met, Wilcoxon signed-rank test was used. For unpaired data sets, unpaired t-test or Mann–Whitney rank-sum test were used for normally and not normally distributed data sets, respectively. Statistical significances in figures are indicated as asterisks: $*P \leq 0.05$, $**P \leq 0.01$, and $***P \leq 0.001$.

Chemicals and drug application

All chemicals were purchased from Sigma (Oakville, ON, Canada). The preparation was continuously superfused with spider saline (in mM: NaCl, 223; KCl, 6.8; $CaCl_2$, 8; $MgCl_2$, 5.1; HEPES, 10; pH 7.8) via plastic tubing with a flow rate of 0.5–1 ml/min (Fig. 1*B*). To avoid turbulence, the superfusion solution was inserted about 3–6 mm from the VS-3 neuron dendrites. The total volume of saline in the recording chamber was 0.3–1 ml. $GABA_A$ receptor agonists and inhibitors of Cl^- transporters were aliquoted and kept frozen until just before each experiment. GABA was initially diluted in distilled water, muscimol in 0.05 M HCl, and bumetanide and furosemide in methanol. About 1 ml of muscimol in 10–500 μM concentrations was used to activate $GABA_A$ receptors in experiments with the cuticular preparation. It was applied via plastic tubing that drained close to the superfusion solution. GABA was used in experiments with the hypodermis preparation and applied using an iontophoretic drug ejection system (MVCS, npi elektronic) to allow rapid local agonist application. Double-barrel borosilicate electrodes with 5- to 15-MΩ resistance were used to allow stray capacitance compensation. The ejecting barrel was filled with 1 M GABA (pH 4.7) and the compensating barrel with 165 mM NaCl. The pipette tip was placed within 50 μm of the soma where GABA was ejected using 0.3- to 1-μA positive-current pulses for 5–10 s. Leakage of GABA from the electrode was prevented by a retaining negative current until ejection. The Cl^- transporter blockers (100 μM bumetanide and 100 μM furosemide) were added to the superfusion solution.

Simulated VS-3 neurons

Simulation of membrane currents in spider VS-3 neurons was based on the Hodgkin–Huxley model (Hodgkin and Huxley 1952), using the exponential Euler method for integrating the differential equations (MacGregor 1987) with a step duration of 20 μs. Full details of the simulation and its responses to step current injections were previously published (Torkkeli and French 2002). The present simulations used parameters identical to those given in the same reference for type A VS-3 neurons. GABA application was simulated by addition of a constant membrane conductance with reversal potential of −30 mV, based on experimental measurement of the reversal potential for GABA simulated current of −27 mV (Panek et al. 2002) and a fitted value of −29.4 mV for simulated GABA application to match experimental step responses (French et al. 2006).

Pseudorandom Gaussian current stimulation was provided by a software 33-bit binary-sequence algorithm clocked to give a bandwidth of 0–300 Hz. Noise amplitude was adjusted to give the desired firing rate of APs. Stimulus data points between the clocked noise values were filled in by linear interpolation. Simulations were run to generate 100 s of membrane potential data, including APs, and then resampled at 10 kHz to generate a simulated voltage recording, which was then processed identically to experimental data.

RESULTS

Muscimol application results in a triphasic response in firing rate when VS-3 neurons are stimulated by mechanical pseudorandom white-noise signals

For mechanical stimulation, pseudorandom white-noise was applied to the VS-3 slits via a stimulating probe, whereas the resulting APs were recorded by an intracellular electrode in the soma of the corresponding VS-3 neuron (Fig. 1*B*; METHODS). When 100 μM muscimol was applied, a membrane depolarization of about 20 mV and a decrease in the AP amplitude were immediately observed (Fig. 2*A*). To investigate AP firing rates under different conditions the original recordings were converted to impulses per second using 1-s-wide bins. Figure 2*B* shows the firing rate of the recording in Fig. 2*A* and a control recording where muscimol was not applied. A triphasic response to muscimol was observed in 22 of the 38 experiments, with an initial increase lasting 5 to 10 s, followed by a decrease lasting 5–50 s, leading to an increase in firing rate that lasted from 200 s to several minutes, often longer than the depolarization and the recording. In seven experiments the response was biphasic (inhibition followed by excitation); in eight experiments only long-lasting excitatory responses were observed and in one experiment only a 10-s inhibitory response was seen. For comparison, a muscimol response of another neuron where the neuron was stimulated with a step mechanical stimuli is shown in Fig. 2*C*. Similar membrane depolarization was observed in response to muscimol as in Fig. 2*A*. However, in this recording only an inhibitory response could be seen at the peak of the depolarization.

We used frequency response analysis to discover whether the muscimol-induced long-lasting excitation that occurred in response to the random stimulation was accompanied by a selective change in sensitivity to different stimulation frequencies. We also asked whether the excitation caused an increase in the signal-to-noise ratio, leading to increased linear information capacity. A 30- to 180-s section of the third phase of each recording with a clear firing rate increase in response to muscimol application was used for analysis. For each neuron,

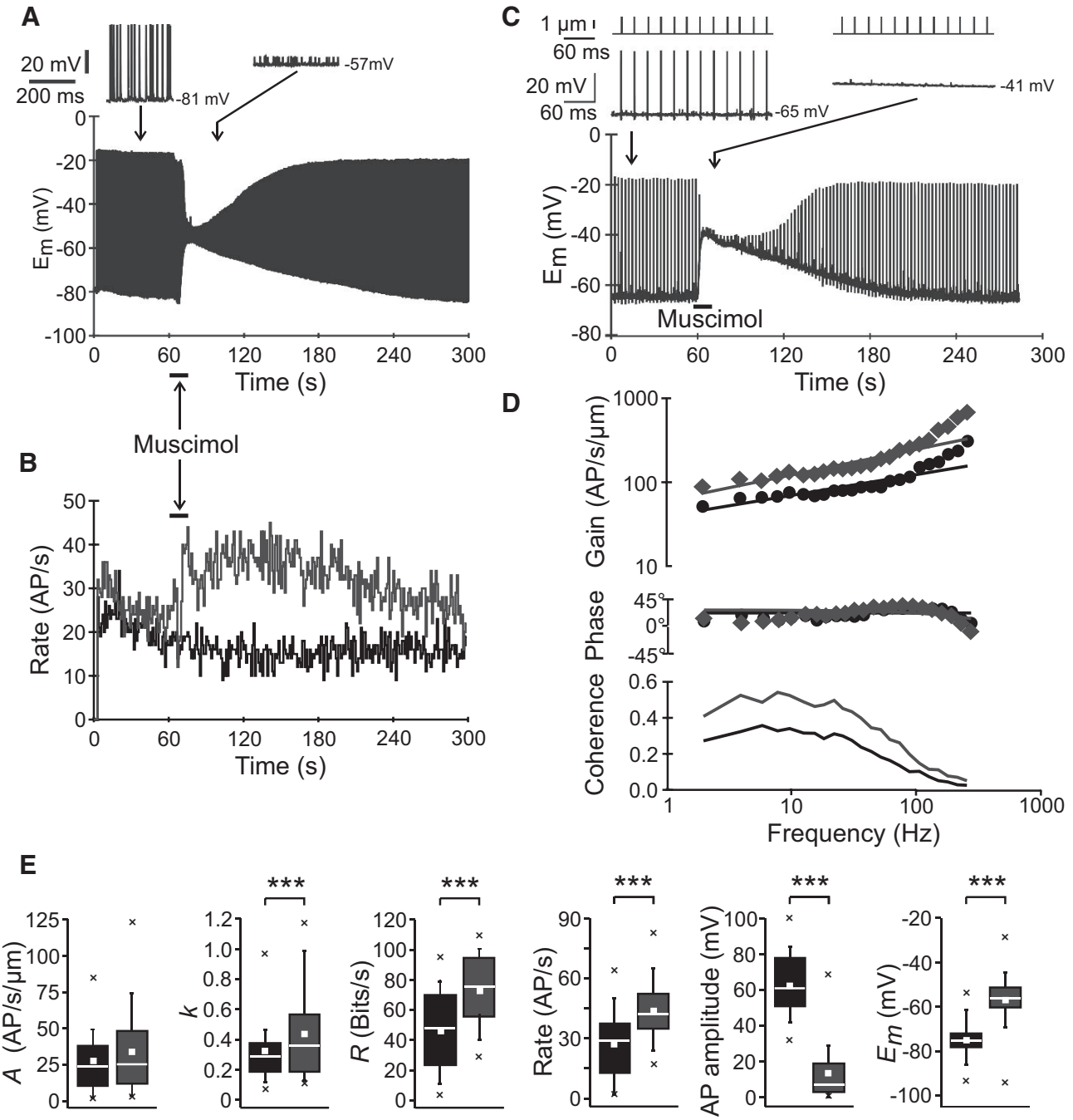

FIG. 2. Muscimol effects on VS-3 neurons during mechanical stimulation. *A*: application of 100 μM muscimol depolarized this neuron by 24 mV. In this recording the neuron was stimulated by pseudorandom white-noise mechanical stimuli (Fig. 1*C*). Action potential (AP) amplitude decreased during depolarization returning slowly to initial level. *Insets* (above) show portions of the same recording at a different scale. *B*: the gray trace shows AP firing rate from the recording in *A* and the black trace is a recording where the same neuron was superfused by normal spider saline. The firing rate in this neuron had a triphasic response to muscimol application with an initial brief increase and decrease followed by a long-lasting increase. The firing rate was calculated using 1-s-wide bins. *C*: for comparison, the neuron in this recording was stimulated with 2-μm mechanical step stimuli at regular intervals while 100 μM muscimol was applied. Muscimol also induced a 24-mV depolarization in this neuron and the AP firing stopped completely during the peak of this depolarization. *D*: frequency response and coherence functions from the long-lasting excitatory phase of the recording in *A*. Solid lines show *Eqs. 1* and *2* fitted to the gain and phase with $k = 0.25$ and 0.29, $A = 39$ and 58 AP$\cdot$s$^{-1}\cdot\mu$m^{-1}, and $\Delta t = 0.02$ and 0.11 ms for the control (black) and muscimol (gray) recordings, respectively. Maximum coherence values were 0.40 and 0.53 and information capacities (*R*) from *Eq. 3* were 50 and 87 bits/s for control (black) and muscimol (gray) recordings, respectively. *E*: box plots compare values from 33 similar experiments obtained under control conditions (black boxes) to those obtained after application of 100 μM muscimol and after the neuron had entered the long-lasting excitatory phase (gray boxes). Parameters of the frequency response functions from *Eqs. 1*, *2*, and *3*. The sensitivity (*A*) was not changed, but the fractional exponent (*k*) and information capacity (*R*) increased significantly after muscimol application. The AP firing rate also increased significantly after muscimol application, whereas AP amplitude decreased significantly. The membrane potential also depolarized significantly in response to muscimol application. Boxes: 25th and 75th percentiles (*bottom* and *top box*, respectively); whiskers: 10th and 90th percentiles (*bottom* and *top whisker*, respectively); horizontal lines indicate the median and the small squares the mean values. Crosses show minimum and maximum outliers.

an initial control recording was performed in normal saline and frequency response analysis was carried out using the same time frame as that for the experiments with muscimol. Figure 2*C* shows an example of estimated gain, phase, and coherence functions for the same neuron as in Fig. 2*A* under control conditions and after muscimol application.

All frequency response functions were well fitted by a power-law relationship (*Eqs. 1* and *2*, METHODS), giving fitted parameters *A* (sensitivity) and *k* (fractional exponent). Information capacity *R* was obtained from the coherence function (*Eq. 3*). Graphical comparisons of these parameters between control and muscimol recordings are shown in Fig. 2*D*. Statistical tests indicated that whereas the parameter *A* was not different, *k* and *R* values were both significantly larger in muscimol-treated neurons compared with the same neurons under control conditions. A larger value of *k* indicates a greater sensitivity to high frequencies and more rapid adaptation. An increase in information capacity *R* was previously observed in spider mechanosensory neurons when the firing rate increased (French et al. 2001; Widmer et al. 2005). Graphical comparisons of AP rate and amplitude as well as membrane potential (E_m) before and after muscimol application are also shown in Fig. 2*D*. Statistical analysis indicated that the AP rate increased significantly, whereas AP amplitude decreased and membrane potential depolarized.

Electrical pseudorandom white-noise stimulation reveals that muscimol has a triphasic effect on firing rate when spikes are initiated in the soma

Previously, mechanically stimulated VS-3 neurons were shown to generate APs in the distal dendrite, close to the stimulation site (Gingl and French 2003; Gingl et al. 2004). To learn whether muscimol-induced changes in firing rate occurred only for dendritic APs, we performed experiments where the VS-3 neuron somata were stimulated directly by the recording electrode. A typical recording with electrical noise stimulation is shown in Fig. 3*A*. Application of 100 μM muscimol induced membrane depolarization and complete inhibition in this neuron. However, when AP firing rates were investigated more closely, a triphasic response to muscimol was observed (Fig. 3*B*). In 15 similar experiments an initial increase lasting 5–10 s was followed by either a complete inhibition or a decrease in spike rate lasting 5–200 s, ending with an increase in firing rate lasting from 200 s to several minutes, often longer than the depolarization and the recording. The background noise level during electrical stimulation prevented inclusion of very small spikes in the analysis, which probably made the complete inhibitory phase seem longer than it really was in some cases and reduced the number of spikes included in the excitatory phase.

Frequency response analysis of the long-lasting excitatory phase of the muscimol response during electrical stimulation experiments showed a statistically significant change in all of the fitted parameters (Fig. 3, *C* and *D*). In addition to *k* and *R*, the sensitivity parameter *A* also increased significantly during the muscimol-induced excitatory phase. The gain increased at all frequencies, but especially at frequencies >10 Hz (Fig. 3*C*). The increase in high-frequency sensitivity caused an increase in signal-to-noise ratio, clearly visible in the coherence plots. Graphical comparisons (Fig. 3*D*) show that, similarly to recordings under mechanical stimulation, application of 100 μM muscimol to electrically stimulated neurons also produced statistically significant changes in firing rate (increase), AP amplitude (decrease), and membrane potential (depolarization).

Dose–response relationships suggest that some parameters are more sensitive to muscimol than others

To investigate the dose–response relationships of the fitted parameters during the excitatory phase of the muscimol response, different concentrations of muscimol were applied to the bath while VS-3 neurons were stimulated mechanically. Changes produced by muscimol were normalized and fitted by the logistic Hill equation (Fig. 4). Changes in variables *A* and *k* at different concentrations were too small and variable to be fitted by this equation. All other variables resulted in Hill coefficients close to unity, indicating that only one molecule of muscimol is required to open the ion channel, similarly to previous results from these neurons (Panek and Torkkeli 2005). The half-maximal muscimol concentration for different variables indicated that a somewhat higher concentration was required to change AP amplitude (EC_{50} = 39.7 μM) and membrane potential (EC_{50} = 43.2 μM) than to change information capacity (EC_{50} = 16.5 μM) or firing rate (EC_{50} = 14.3 μM). Previously, an EC_{50} of 15 μM was obtained for muscimol-induced membrane potential change in VS-3 neurons (Panek and Torkkeli 2005). This lower number is probably due to the fact that the previous experiments were done using the hypodermis preparation, where drug access to the neurons is better than that in the cuticular preparation used here.

Depolarization without muscimol has effects similar to those of muscimol application on spike rate and frequency response parameters

Depolarization in response to GABA or muscimol in VS-3 neurons is a major contributor to inhibition of AP firing response to step stimuli (French et al. 2006; Panek et al. 2008). To test whether depolarization also contributed to the excitatory response when random white-noise stimulation was used, we depolarized cell membranes by injecting positive current in the VCcCC mode. This method allows compensation of slow membrane potential changes without affecting faster voltage responses, such as APs (Sutor et al. 2003). This method allowed us to separate conductance-based changes from voltage-driven changes. A typical result of this type of experiment is shown in Fig. 5*A*, where current injection depolarized the neuron, causing a clear increase in the firing rate (Fig. 5*B*). No inhibition was observed in any of the 12 similar experiments. When experimental parameters from all similar experiments were compared with parameters obtained from control recordings without depolarization, a statistically significant difference was detected in the information capacity, firing rate, and AP amplitude (Fig. 5*C*). No significant changes were detected in parameters *A* or *k*.

We also compared responses to depolarization alone to those obtained from experiments where 100 μM muscimol was used (Table 1). Although changes in parameters *A*, *k*, *R*, and firing rate were all smaller in depolarization experiments, the changes were not statistically significantly different from those with muscimol, although the reduction in AP amplitude was significantly larger in muscimol experiments. This is also clearly visible in the *insets* to Figs. 2*A* and 5*A*, indicating that the typical strong

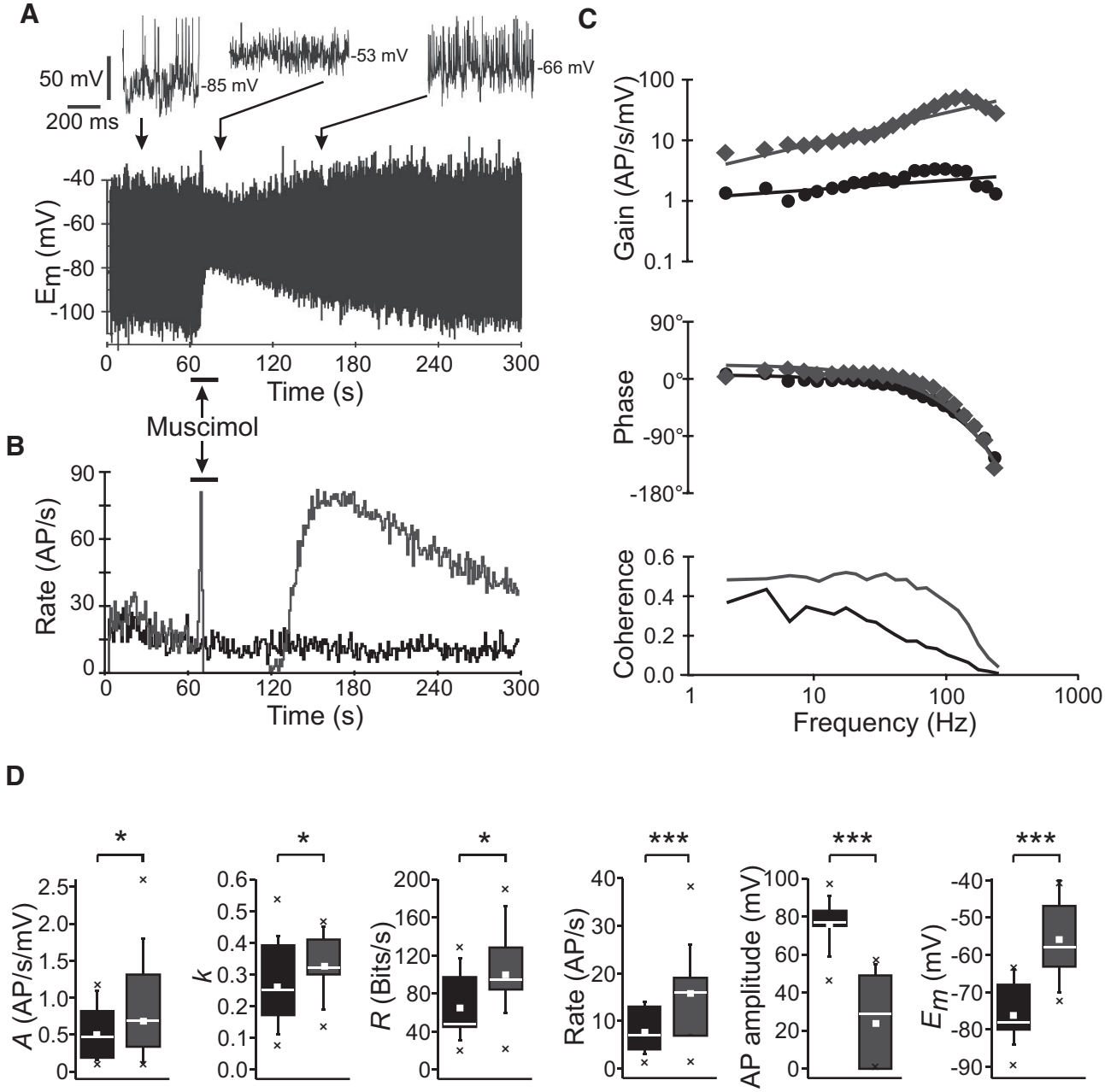

FIG. 3. Muscimol effects on a VS-3 neuron stimulated electrically with pseudorandom white noise. *A*: this neuron depolarized by 32 mV in response to application of 100 μM muscimol. *B*: gray trace shows firing rate when muscimol was applied (same recording as in *A*) and the black trace is the firing rate of the same neuron under control conditions. A triphasic change in rate was observed in response to muscimol application with initial increase, then inhibition, ending in long-lasting excitation. *C*: frequency response and coherence functions for the long-lasting excitatory period of the experiment shown in *A*. Solid lines show *Eqs. 1* and *2* fitted to the gain and phase with $k = 0.08$ and 0.25, $A = 1.1$ and 1.7 impulses$\cdot s^{-1}\cdot mV^{-1}$, $\Delta t = 1.64$ and 1.90 ms for the control (black) and muscimol (gray) recordings, respectively. Maximum coherence values were 0.47 and 0.50 and information capacities (R) from *Eq. 3* were 52 and 136 bits/s for control (black) and muscimol (gray) recordings, respectively. *D*: box plots compare values from 15 similar experiments as in *A* under control conditions (black boxes) to those after application of 100 μM muscimol (gray boxes). Parameters of the frequency response function calculated from *Eqs. 1*, *2*, and *3*. The sensitivity A, fractional exponent k, and information capacity R all increased significantly in response to muscimol. The firing rate also increased significantly, whereas AP amplitude decreased significantly. Membrane potential depolarized significantly after muscimol application. Box plots as in Fig. 2.

shunting effect that occurs when muscimol is applied did not occur when the neurons were depolarized without muscimol application.

Firing rate and frequency response parameters increased in response to muscimol application when depolarization was prevented

By clamping the membrane potential to the resting level in the VCcCC mode we were able to investigate the effects of 100 μM muscimol on firing when depolarization was prevented. Figure 6*A* shows a typical recording from a VS-3 neuron stimulated mechanically in VCcCC mode while 100 μM muscimol was applied. There was a clear decrease in the AP amplitude, even though the membrane did not depolarize. A brief excitatory response, followed by an inhibitory response, and ending in a long-lasting excitatory response in AP firing were observed in all five experiments (Fig. 6*B*), similarly to responses

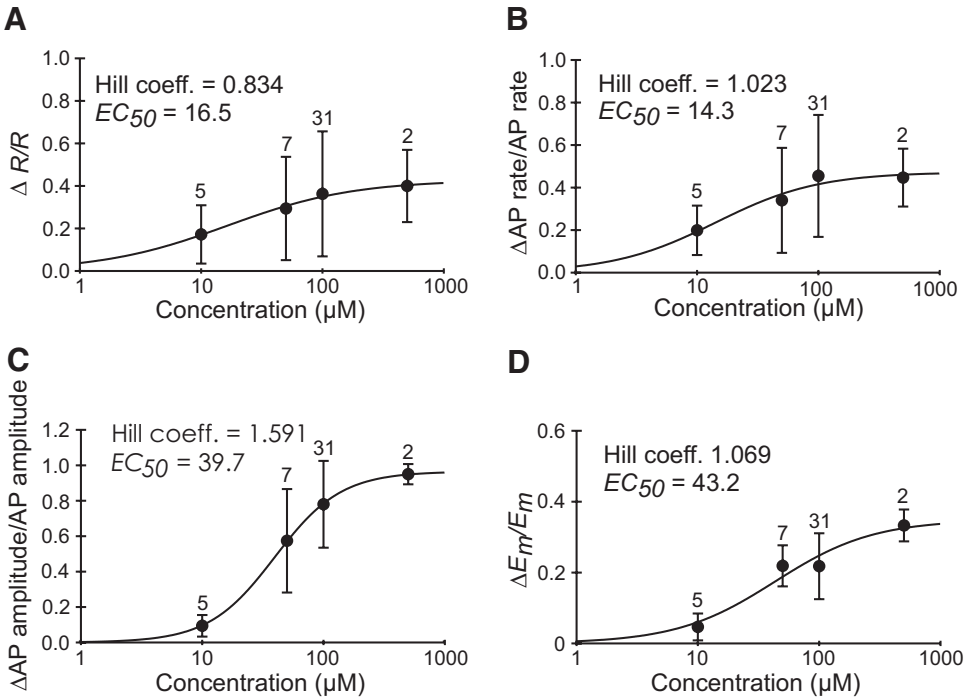

FIG. 4. Dose–response relationships of muscimol effects on parameters recorded during mechanical pseudorandom noise stimulation. All parameters were normalized and plotted against muscimol concentration. *A*: dose–response relationship of information capacity *R*. *B*: AP firing rate. *C*: AP amplitude. *D*: peak change in membrane potential after muscimol application. The data were fitted with the logistic Hill equation ($Y = Y_{max}[C]^n/([C]^n + [EC_{50}]^n)$, where Y is response, Y_{max} is maximal response, $[C]$ is agonist concentration, $[EC_{50}]$ is the half-maximal effective concentration, and n is the Hill coefficient. Results are shown as means ± SD with the number of experiments indicated above each symbol.

in normal current-clamp mode when muscimol was applied (Fig. 2*B*). There were no differences in the variable *k* between control and muscimol recordings, but the sensitivity *A*, information capacity *R*, and firing rate were significantly higher and AP amplitude was significantly lower in recordings with muscimol than under control conditions (Fig. 6*C*).

When the changes in parameters obtained from experiments where depolarization was prevented in VCcCC mode during muscimol application were compared with those changes that occurred when depolarization was allowed to occur, there were no statistically significant differences in any of the parameters (Table 1). Therefore when depolarization was prevented while muscimol was applied, the excitatory response remained intact, suggesting that either shunting alone was adequate to cause the response or that shunting may have been more local than the depolarization.

Simulated VS-3 neurons can predict the excitatory effect of GABA

Simulations were used to separate the depolarization and shunting effects of treatment with $GABA_A$ receptor agonists (Fig. 7). Random current amplitude was chosen to give a similar mean firing rate to electrically stimulated neurons (compare with Fig. 3). Then, GABA conductance was adjusted to give a similar increase in firing rate to the mean increase seen experimentally when 100 μM muscimol was applied. Frequency response functions from simulated data were well fitted by the power law (*Eqs. 1* and *2*). Fitted parameters for simulations with GABA conductance changed in the same directions as the experimental values, with the exception of the parameter *A*, which decreased by a small amount instead of increasing. The depolarizing effect of GABA was simulated by adding a constant depolarizing current to give the same change in membrane potential. The shunting effect of GABA was simulated by adding conductance to the leak component of the model. Depolarization produced closely similar effects to muscimol in all parameters (compare with Fig. 3). Conversely, increased shunting produced very small changes in all parameters, usually in the opposite direction to muscimol application. However, shunting reduced the model membrane time constant from 16.8 to 9.2 ms.

Blocking cation–chloride cotransporter function reduced GABA induced depolarization, but had no effect on the increase in firing rate

The polarity of GABAergic neurotransmission depends mainly on the intracellular $[Cl^-]$ that, in neurons, is regulated by cation–chloride cotransporters. Depolarizing responses to GABA and muscimol are believed to be caused by a relatively high intracellular $[Cl^-]$ (Alvarez-Leefmans et al. 1998; Cheung et al. 2006; Payne et al. 2003) and thus mediated by NKCC1, a Na^+-K^+-Cl^- cotransporter that accumulates Cl^- in cells (Cheung et al. 2006; Payne et al. 2003). Inhibitors of this transporter have been shown to suppress excitatory GABA responses in several vertebrate and invertebrate preparations (Cheung et al. 2006; Choi et al. 2008; Dzhala et al. 2005; Sipilä et al. 2006). To learn whether the excitatory GABA response in VS-3 neurons could also be regulated by Cl^- transporters we used the "loop" diuretics furosemide and bumetanide. In addition to NKCC1 these diuretics also inhibit KCC1, a K^+-Cl^- cotransporter that actively extrudes Cl^- from cells in vertebrate and invertebrate preparations (Cheung et al. 2006; Deisz and Lux 1982; Gillen et al. 2006; Hille and Walz 2006; Ianowski and O'Donnell 2004; Theander et al. 1999). Furosemide has about equal potency for NKCC1 and KCC1, but bumetanide has a significantly higher affinity for NKCC1 (Payne et al. 2003) and would therefore be more likely to affect the response of VS-3 neurons. We tested both antagonists on the GABA response of VS-3 neurons. These experiments were performed using the hypodermis preparation of a VS-3 organ

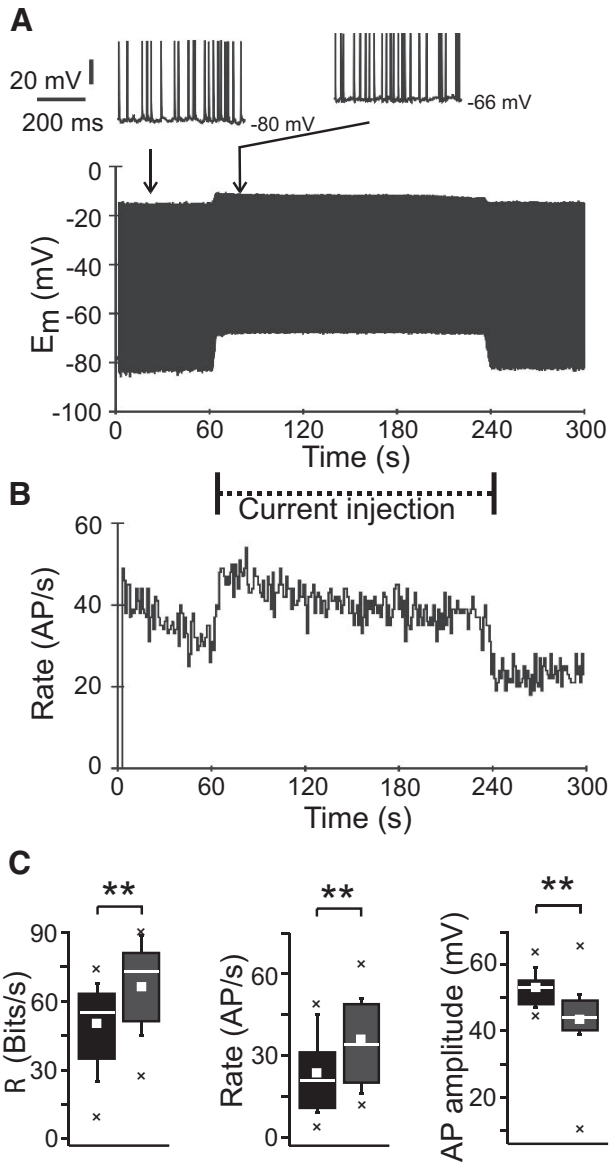

FIG. 5. Effects of depolarization without muscimol application on VS-3 neurons. *A*: a typical recording in voltage-clamp–controlled current-clamp mode (VCcCC) where current injection depolarized the neuron by 14 mV. AP amplitude decreased from 65 to 54 mV during depolarization (*insets*). *B*: there was a clear increase in firing rate during the depolarization. *C*: box plots comparing parameters during the excitatory period recorded from 11 experiments with current injection (gray boxes) to parameters recorded under control conditions (black boxes). The neurons depolarized by 12.9 ± 3.5 mV (mean ± SD). There was a significant increase in the information capacity (*R*) during depolarization. Firing rate also increased significantly, whereas AP amplitude decreased significantly. Box plots as in Fig. 2.

where the organ is removed from the cuticle, allowing relatively easy access by the antagonists to the neurons. GABA was ejected iontophoretically close to the neurons.

A total of 21 experiments were performed using this preparation. In 6 experiments the response to GABA was triphasic: 5- to 10-s excitatory phase followed by a 50- to 200-s inhibitory phase and ending in an excitatory phase lasting from 200 s to several minutes, often exceeding the recording period. In 15 experiments only the inhibitory and excitatory phases were present. Figure 8*A* shows the firing rate of a VS-3 neuron under control conditions, when GABA was ejected while the neuron was superfused in normal saline and when GABA was ejected while the neuron was superfused in saline supplemented with 100 μM furosemide for 15 min. Figure 8*B* shows AP firing rates from a similar series of experiments, but with the saline supplemented by 100 μM bumetanide for 20 min. In both experiments with normal saline, GABA ejection initially inhibited but then induced a significant increase in firing rate. These effects were unchanged when either of the transporter antagonists was used.

Table 2 shows parameters obtained during the excitatory period from several similar experiments as in Fig. 8. There were no differences in parameters *A*, *k*, or *R* after GABA ejection with either of the antagonists compared with similar GABA ejection in normal saline. The firing rate was somewhat lower when furosemide was present and the membrane potential was slightly more negative when either of the antagonists was present. However, these changes were not statistically significant. Peak membrane potential after GABA-induced depolarization was more negative when either of the transporters was present, but only the value with bumetanide was significantly different compared with the control. These results suggest that although GABA application probably affects Cl^- transport in VS-3 neurons via the NKCC1 transporter, it does not have significant effects on firing rate during the time frame used in our experiments.

DISCUSSION

Our main finding was that when VS-3 neurons were stimulated with randomly varying signals their response to GABA and muscimol was usually triphasic, consisting of a brief excitation, followed by inhibition, and ending with a long-lasting excitation. It would be difficult to replicate the strains and vibrations that naturally excite these neurons, but stimulation with random signals provides a wide range of frequencies and amplitudes, giving a closer approximation to natural stimulation than deterministic step or sinusoidal stimuli. In previous experiments using step electrical stimuli, VS-3 neurons were inhibited by GABA and muscimol, whereas the same agonists had a smaller effect on mechanically stimulated neurons (Gingl et al. 2004; Panek et al. 2002). Our current results indicate that the VS-3 neuron response to these agonists is much more complex with random stimulation. Under these conditions, excitation was much more prominent and longer lasting than inhibition. Although many mechanosensory neurons respond to complex stimuli, it is possible that in some cases deterministic stimuli are closer to natural stimuli than white noise. Therefore each type of neuron would need to be tested using stimulation that is most appropriate to the natural conditions of the particular neuron.

Frequency response and coherence function measurements revealed that the neurons' overall sensitivity, selectivity for frequencies >10 Hz, and information capacity increased during the long-lasting excitatory phase. Increased high-frequency responses were clearer in the data obtained from electrical stimulation than those obtained from mechanical stimulation, probably due to the more limited frequency range of the servo-controlled mechanical stimulator (see METHODS). Lack of mechanical higher-frequency stimulation components reduces the signal-to-noise ratio and coherence at high frequencies

TABLE 1. *Comparison of the changes in experimental values recorded under various conditions*

Variable	Condition			*P* Value	
	1) 100 μM Muscimol	*2*) Depolarization, No Muscimol	*3*) No Depolarization, 100 μM Muscimol	*1* vs. *2*	*1* vs. *3*
A, AP·s^{-1}·μm^{-1}	8.90 ± 20.50	0.20 ± 14.60	15.30 ± 11.20	0.425	0.1980
k	0.11 ± 0.15	0.07 ± 0.11	0.01 ± 0.07	0.374	0.0849
R, bits/s	26.90 ± 18.60	15.80 ± 15.20	24.40 ± 10.60	0.0665	0.7679
Rate, AP/s	17.10 ± 13.80	12.40 ± 9.00	18.60 ± 18.80	0.1907	0.8579
AP amplitude, mV	71.50 ± 12.50	8.80 ± 11.00	35.20 ± 13.30	<0.0001	0.1352
n	38	12	5		

Values in each cell are means ± SD. Conditions: *1*) when 100 μM muscimol was applied under regular current-clamp without current injection; *2*) when neurons were depolarized under VCcCC and no muscimol was applied; *3*) when the depolarization was prevented under VCcCC while 100 μM muscimol was applied. *A,* sensitivity; *k*, fractional exponent; *R*, information capacity; AP, action potential; *n*, number of experiments.

(French et al. 2001). This is a common problem in experimental work involving mechanical stimulation.

In spite of this limitation, our results clearly showed that membrane depolarization by muscimol or GABA was accompanied by increased AP firing rates and increased sensitivity to high frequencies. This raises the following questions: What are the mechanisms that cause these effects? What are their physiological consequences? What is the general relevance of our results?

Depolarization, shunting, and GABA-induced excitation

Membrane depolarization and increased conductance (shunting) have been previously shown to contribute to the inhibitory effects of GABA, including presynaptic inhibition, on primary afferent mechanosensory neurons in many vertebrate and invertebrate preparations (Cattaert and El Manira 1999; Rudomin and Schmidt 1999). Since similar depolarization and shunting occur in the peripheral parts of spider VS-3 neurons and have previously been shown to contribute to the inhibitory effect (French et al. 2006; Panek et al. 2002), we asked whether they could also explain the increase in sensitivity when the neurons are stimulated with random signals. When VS-3 neurons were clamped to a depolarizing potential, similar to that observed during muscimol application, their firing rate and information capacity increased in the same way as that in experiments where muscimol was applied, even without shunting. However, when neurons were prevented from depolarizing while muscimol was applied but shunting did occur the excitatory response remained. This latter finding was unexpected since it is unlikely that a change in membrane conductance alone would lead to increased firing. This finding was also not shown by the simulated neurons. A possible explanation is that the voltage-clamp was limited to the neuron's cell body and nearby regions, whereas muscimol was still able to depolarize more remote regions, especially including the sensory dendrite, where action potentials are initiated (Gingl and French 2003; Gingl et al. 2004).

The VS-3 neuron simulation has previously been used to estimate the relative contributions of shunting and inactivation to the inhibitory effect of GABA (French et al. 2006). Simulated neurons depolarized and increased their firing rate when GABA current was added to random-noise stimulation, similarly to experimental neurons. The simulations gave good agreement with experimental neurons for depolarization, except for the sensitivity *A*, which changed by a small amount in the opposite direction to the experimental mean value. Other parameters from the simulated power-law fittings increased similarly to experiments. Depolarization closely mimicked GABA application, but shunting did not. Because of the reduction in the model membrane time constant, shunting might be expected to somewhat affect neuronal firing. However, the relatively large conductance changes produced by voltage-activated currents when the neuron is firing APs probably reduce the importance of this shunting effect. In contrast, relatively small depolarizations are able to significantly shift the activation and inactivation parameters of these currents. Therefore the simulations suggest that the depolarizing role of GABA dominates its effects on VS-3 neurons stimulated by randomly varying membrane current. This finding is consistent with a previous report where a simulated model of spinal cord neurons revealed that shunting was a local effect while the depolarization was longer lasting, spreading electrotonically in the somatodendritic tree leading to excitation (Jean-Xavier et al. 2007).

In the real VS-3 neurons, the excitatory effect often lasted significantly longer than depolarization, suggesting that factors other than depolarization contribute to this effect. In addition, the depolarization experiments did not produce the increase in relative sensitivity to high frequencies, suggesting that this effect may also be partly caused by other mechanisms elicited by GABA or muscimol. The VS-3 neuron intracellular [Ca^{2+}] was previously shown to increase significantly when GABA was applied (Panek et al. 2008). It is possible that this Ca^{2+} rise could lead to changes in membrane permeability that may contribute to the excitatory effect.

Chloride transporters do not reduce the excitatory effect of GABA

The Na^+-K^+-Cl^- cotransporter NKCC1 accumulates Cl^- in cells and maintains the relatively high Cl^- gradient required for a depolarizing GABA response (Payne et al. 2003). This secondary active transporter is also responsible for the high intracellular Cl^- gradient in amphibian dorsal root ganglion neurons and Rohon–Beard neurons, which respond to $GABA_A$ receptor activation with depolarization (Alvarez-Leefmans et al. 1988, 2001; Rohrbough and Spitzer 1996). Consistent with previous studies, bumetanide reduced the GABA-induced membrane depolarization in VS-3 neurons by 6.7 mV. For example, tadpole Rohon–Beard neuron reversal potential for GABA was about 10 mV (Rohrbough and Spitzer 1996) and rat hippocampal neurons about 18 mV more negative after bumetanide treatment (Sipilä et al. 2006). In previous studies

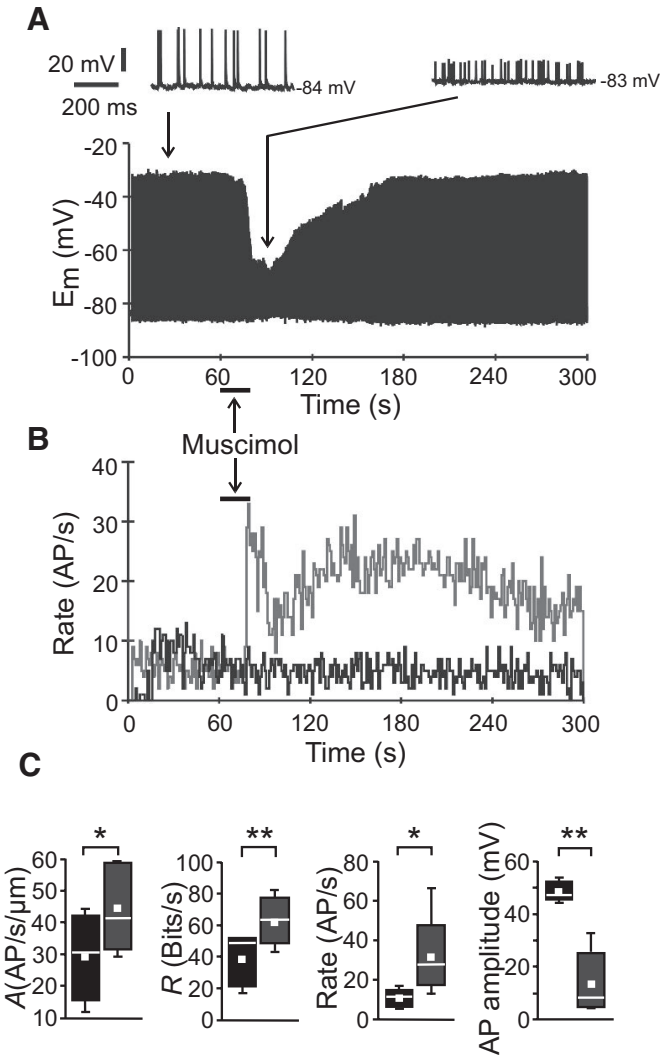

FIG. 6. Muscimol effects on mechanically stimulated VS-3 neurons when somatic membrane depolarization was prevented in VCcCC mode. *A*: an original recording shows that although the membrane potential was clamped to −84 mV, the spike amplitude decreased from 44 to 8 mV in response to application of 100 μM muscimol. *B*: the AP firing rate had a triphasic response ending in long-lasting excitation (black, control; gray, muscimol). *C*: box plots from 5 recordings compare control recordings in VCcCC mode (black boxes) to the excitatory phase in recordings where 100 μM muscimol was applied (gray boxes). The sensitivity *A*, information capacity *R*, and AP firing rate all increased, whereas the AP amplitude decreased. Box plots as in Fig. 2.

bumetanide treatment has also been shown to inhibit spontaneous excitatory bursts in rat pyramidal and hippocampal neurons (Choi et al. 2008; Dzhala et al. 2005; Sipilä et al. 2006). A significant decrease in spontaneous firing was also observed in *Lymnaea stagnalis* neurons, together with a hyperpolarizing effect on the resting membrane potential (Cheung et al. 2006). We found that the bumetanide-induced reduction of membrane depolarization in VS-3 neurons was not accompanied by a significant effect on firing rate during 6 min of random-noise stimulation. A much longer lasting stimulation followed by even larger reduction of depolarization may be required to significantly alter the firing behavior of these neurons.

It is also possible that the spider VS-3 neurons use Cl^- transporters different from those of most other species and that these transporters are not sensitive to bumetanide or furosemide. However, this is unlikely since both antagonists have previously been extensively used in many other invertebrate species, including *Drosophila* (Ianowski and O'Donnell 2004), moth (Gillen et al. 2006), cockroach (Hille and Waltz 2006), crayfish (Deisz and Lux 1982), and lobster (Theander et al. 1999), suggesting that similar Cl^- transporters in a number of different species are sensitive to these drugs. However, it is also important to remember that in addition to Cl^-, ionotropic GABA receptor channels are permeable to other anions, such

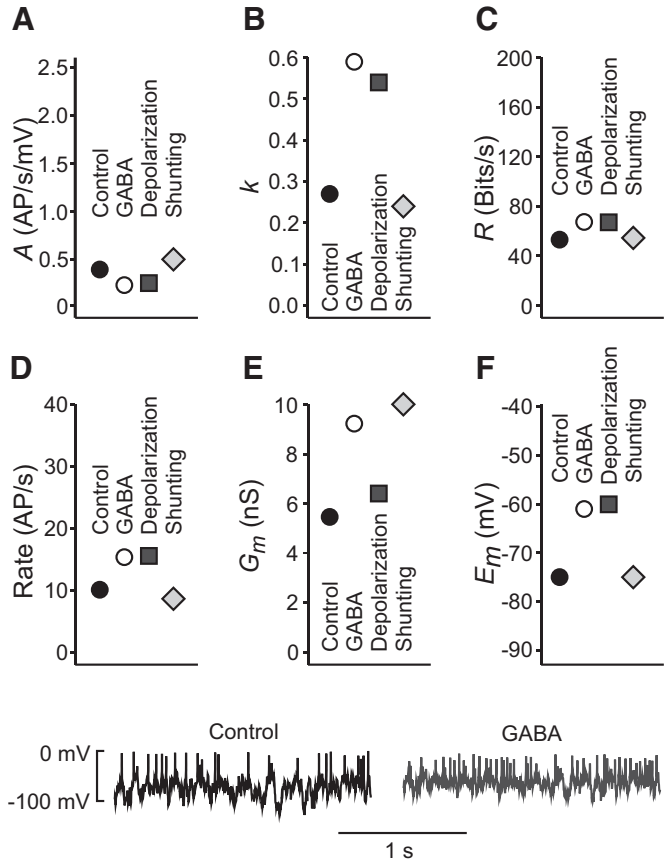

FIG. 7. Simulations of a VS-3 neuron stimulated by random electric current. Results of responses to current stimulus of 0.4 nA rms under 4 different conditions: control (black circles), GABA application (white circles), membrane depolarization (dark gray squares), and membrane shunting (light gray diamonds). In each case, the membrane potential recorded from a simulated period of 100 s was processed by the same software and procedures as the experimental data. Results are presented on plots similar to those of Fig. 3 for comparison with experiments. *A*: sensitivity at 1 Hz, *A*. *B*: fractional exponent, *k*. *C*: information capacity, *R*. *D*: firing rate. *E*: membrane conductance at the resting potential, G_m. *F*: membrane potential, E_m. GABA conductance (3 nS) was chosen to give a similar range of firing rates to the experiments (10.1 impulses/s increasing to 15.3 impulses/s). Depolarizing current (0.1 nA) gave a similar membrane potential (−60 mV) to that produced by simulated GABA treatment (−61 mV). Shunting (4.6 nS) gave a similar resting membrane conductance G_m, (10.0 nS) to that produced by GABA treatment (9.2 nS). Simulated GABA application produced changes similar to those seen experimentally, except for the sensitivity parameter *A*, which decreased slightly. Firing rate increased, fractional exponent (*k*) increased, information capacity increased, and the membrane depolarized. Simulated depolarization alone produced changes in all parameters similar to those seen with simulated GABA application. In contrast, simulated shunting alone produced, at most, small changes in the opposite direction for each parameter. *Insets* below show samples of raw data from control and GABA-treated simulations subjected to the same random input current. Note the depolarization and increased firing rate produced by GABA.

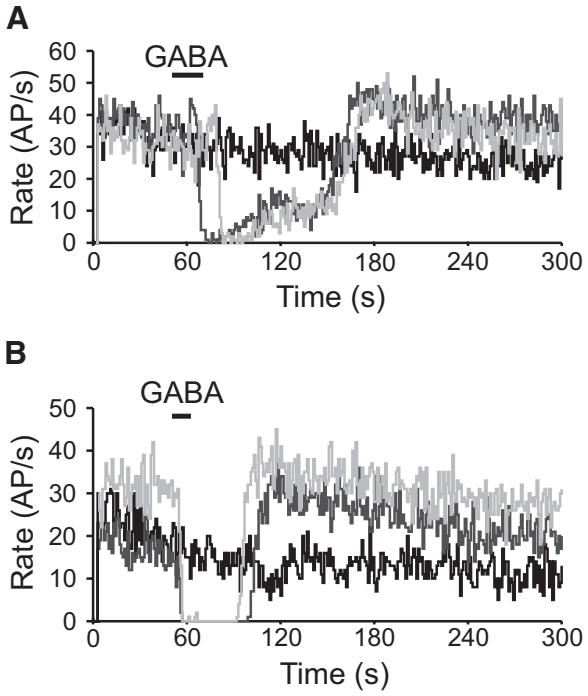

FIG. 8. Cation–chloride cotransporter antagonists did not reduce the inhibitory or excitatory effect of GABA. *A*: firing rate of a VS-3 neuron under control conditions (black). When GABA was applied iontophoretically and the neuron was superfused by normal saline (dark gray) this neuron responded with an initial inhibition followed by an excitation. When 100 μM furosemide was added to the superfusion solution, GABA application had a similar biphasic effect on this neuron (light gray) as in normal saline. *B*: firing rate under control conditions (black), when GABA was ejected iontophoretically while the cells were in normal saline (dark gray), and when GABA was applied while 100 μM bumetanide was in the bath solution (light gray). Firing rate was similar with and without bumetanide in the bath. Period of GABA ejection is indicated above each image.

as HCO_3^- (Alvarez-Leefmans et al. 1998; Kaila and Voipio 1990). So, mechanisms linked to Cl^- transport constitute only one possibility that could produce the effects observed here and a better understanding of the ionic mechanisms involved would be needed to fully determine how the excitatory effect is generated.

Physiological significance of GABA effects on VS-3 neurons and the general relevance of our findings

The inhibitory effect of GABA on primary afferent mechanosensory neurons is thought to be important for suppressing less important signals from the large number of inputs that are continuously received by the CNS from various sense organs. Abolishing unwanted signals at an early stage, before they ever reach the CNS, could be an economical way of dealing with this situation (Rudomin and Schmidt 1999). Arachnids and crustaceans, which have complex networks of efferent synaptic contacts onto the most peripherally located parts of their mechanosensory neurons (Elekes and Florey 1987; Fabian-Fine et al. 1999, 2002; Torkkeli and Panek 2002), have the opportunity to suppress or enhance afferent signals at the earliest stages. Peripheral modulation also occurs in vertebrate muscle spindles and the outer hair cells in the ear, but it is probably a more general phenomenon, as shown by the sensitivity of some vertebrate mechanoreceptors to sympathetic activity (Loewenstein 1956), GABAergic inhibition of vagal mechanoreceptors (Page and Blackshaw 1999), and the presence of $GABA_A$ receptors on cat primary afferent terminals (Carlton et al. 1999). Our findings indicate that even with only one transmitter and one type of receptor, modulation of sensory signals may be dramatically different in different circumstances. GABA may inhibit repetitive signals appearing at low frequencies but enhance inputs that change rapidly, carrying higher frequencies. This could be an effective and economical way of prioritizing input information and similar systems could be used by the other transmitters that modulate mechanosensitive neurons.

In our experiments, the increased firing rate with GABA or muscimol was accompanied by a reduction in AP amplitude. With mechanical stimulation these APs are generated in the dendrite and they propagate for long distances through the soma to the axon terminals in central ganglia. In living animals, GABA release is probably local—shunting a small area of the membrane—and APs will be regenerated to full amplitude as they travel toward the axon terminals. Even if GABA release occurred in the axon terminals, as in presynaptic inhibition (e.g., Clarac and Cattaert 1996; Rudomin and Schmidt 1999), an increased spike rate could still result in additional transmitter release and an excitatory effect on the postsynaptic neuron. Information transmission via APs is generally based on spike timing rather than amplitude. However, confirmation of the postsynaptic effects of GABA will probably require direct recordings from central neurons.

The most important conclusion from these experiments is that the effects of a modulating transmitter like GABA on AP encoding can vary profoundly depending on the nature of the signal being encoded. Using simple, deterministic stimuli to

TABLE 2. *Comparison of parameters obtained from VS-3 neurons when superfused by spider saline while GABA was applied iontophoretically (control) to values obtained from similar experiments when 100 μM furosemide or 100 μM bumetanide were added to the superfusion solution*

Parameter	Control	Furosemide	*P*	Control	Bumetanide	*P*
A, imp·s^{-1}·mV^{-1}	0.12 ± 0.05 (6)	0.10 ± 0.02 (6)	0.1259	0.07 ± 0.05 (7)	0.07 ± 0.04 (7)	0.8868
k	0.21 ± 0.04 (6)	0.19 ± 0.04 (6)	0.1580	0.29 ± 0.14 (7)	0.29 ± 0.16 (7)	0.8570
R, bits/s	94.90 ± 29.00 (6)	98.90 ± 14.60 (6)	0.6843	84.80 ± 48.60 (7)	90.70 ± 41.70 (7)	0.7153
Rate, AP/s	24.60 ± 10.10 (6)	19.60 ± 6.80 (6)	0.0876	13.60 ± 10.20 (7)	13.90 ± 10.40 (7)	0.8519
E_m before GABA, mV	−69.10 ± 3.80 (8)	−71.40 ± 4.40 (8)	0.1218	−67.80 ± 6.20 (13)	−71.90 ± 5.10 (13)	0.0799
E_m peak after GABA, mV	−49.80 ± 7.80 (8)	−52.00 ± 7.50 (8)	0.2242	−48.50 ± 9.90 (13)	−55.20 ± 12.60 (13)	0.0348

Values in each cell are means ± SD, with the number of experiments in parentheses. *A*, sensitivity; *k*, fractional exponent; *R*, information capacity; AP, action potential; E_m, membrane potential. *P* values indicate that the peak membrane potential after GABA ejection was significantly more negative with bumetanide treatment, but there were no statistically significant differences in any other parameters.

assess neural function or the effects of modulation may not provide a reliable description of normal physiology in many vertebrate and invertebrate neural systems. In systems where behaviorally generated naturalistic stimuli have been used, such as insect visual systems, neurons have been shown to be able to extract behaviorally important information that was not detectable when conventional visual stimuli were used (Kern et al. 2005; Lindemann et al. 2005). Although random white-noise stimulation allowed us to test the VS-3 neuron GABA response under a wide range of frequencies, it would be more desirable to generate naturalistic stimuli that correspond to the movements that excite VS-3 neurons in real life and test the neurons' response to GABA and other transmitters under these conditions.

ACKNOWLEDGMENTS

We thank S. Meisner for expert technical assistance and animal care and M. Woodin for advice on the chloride cotransporter experiments.

GRANTS

This work was funded by Canadian Institutes of Health Research, Nova Scotia Health Research Foundation, and Dalhousie Medical Research Foundation.

REFERENCES

Alvarez-Leefmans FJ, Leon-Olea M, Mendoza-Sotelo J, Alvarez FJ, Anton B, Garduno R. Immunolocalization of the Na^+-K^+-$2Cl^-$ cotransporter in peripheral nervous tissue of vertebrates. *Neuroscience* 104: 569–582, 2001.

Alvarez-Leefmans FJ, Nani A, Marguez S. Chloride transport, osmotic balance, and presynaptic inhibition. In: *Presynaptic Inhibition and Neural Control*, edited by Rudomin P, Romo R, Mendell LM. New York: Oxford Univ. Press, 1998, p. 50–79.

Barth FG. *A Spider's World: Senses and Behavior*. Heidelberg, Germany: Springer-Verlag, 2001.

Barth FG, Libera W. Ein Atlas der Spaltsinnesorgane von *Cupiennius salei* Keys, Chelicerata (Aranea). *Z Morphol Tiere* 68: 343–369, 1970.

Ben Ari Y. Excitatory actions of GABA during development: the nature of the nurture. *Nat Rev Neurosci* 3: 728–739, 2002.

Bendat JS, Piersol AG. *Engineering Applications of Correlation and Spectral Analysis*. New York: Wiley, 1980.

Carlton SM, Zhou S, Coggeshall RE. Peripheral $GABA_A$ receptors: evidence for peripheral primary afferent depolarization. *Neuroscience* 93: 713–722, 1999.

Cattaert D, El Manira A. Shunting versus inactivation: analysis of presynaptic inhibitory mechanisms in primary afferents of the crayfish. *J Neurosci* 19: 6079–6089, 1999.

Cheung U, Moghaddasi M, Hall HL, Smith JJ, Buck LT, Woodin MA. Excitatory actions of GABA mediate severe-hypoxia-induced depression of neuronal activity in the pond snail (*Lymnaea stagnalis*). *J Exp Biol* 209: 4429–4435, 2006.

Choi HJ, Lee CJ, Schroeder A, Kim YS, Jung SH, Kim JS, Kim DY, Son EJ, Han HC, Hong SK, Colwell CS, Kim YI. Excitatory actions of GABA in the suprachiasmatic nucleus. *J Neurosci* 28: 5450–5459, 2008.

Clarac F, Cattaert D. Invertebrate presynaptic inhibition and motor control. *Exp Brain Res* 112: 163–180, 1996.

Cooley JW, Tukey JW. An algorithm for the machine calculation of complex Fourier series. *Math Comput* 19: 297–301, 1965.

Deisz RA, Lux HD. The role of intracellular chloride in hyperpolarizing post-synaptic inhibition of crayfish stretch receptor neurones. *J Physiol* 326: 123–138, 1982.

Dzhala VI, Talos DM, Sdrulla DA, Brumback AC, Mathews GC, Benke TA, Delpire E, Jensen FE, Staley KJ. NKCC1 transporter facilitates seizures in the developing brain. *Nat Med* 11: 1205–1213, 2005.

Elekes K, Florey E. New types of synaptic connections in crayfish stretch receptor organs: an electron microscopic study. *J Neurocytol* 16: 613–626, 1987.

Fabian-Fine R, Höger U, Seyfarth E-A, Meinertzhagen IA. Peripheral synapses at identified mechanosensory neurons in spiders: three-dimensional reconstruction and GABA-immunoreactivity. *J Neurosci* 19: 298–310, 1999.

Fabian-Fine R, Seyfarth E-A, Meinertzhagen IA. Peripheral synaptic contacts at mechanoreceptors in arachnids and crustaceans: morphological and immunocytochemical characteristics. *Microsc Res Tech* 58: 283–298, 2002.

French AS, Höger U, Sekizawa S-I, Torkkeli PH. Frequency response functions and information capacities of paired spider mechanoreceptor neurons. *Biol Cybern* 85: 293–300, 2001.

French AS, Holden AV. Alias-free sampling of neuronal spike trains. *Kybernetik* 8: 165–171, 1971.

French AS, Panek I, Torkkeli PH. Shunting versus inactivation: simulation of GABAergic inhibition in spider mechanoreceptors suggests that either is sufficient. *Neurosci Res* 55: 189–196, 2006.

French AS, Torkkeli PH, Seyfarth E-A. From stress and strain to spikes: mechanotransduction in spider slit sensilla. *J Comp Physiol A Sens Neural Behav Physiol* 188: 739–752, 2002.

Gillen CM, Blair CR, Heilman NR, Somple M, Stulberg M, Thombre R, Watson N, Gillen KM, Itagaki H. The cation–chloride cotransporter, masBSC, is widely expressed in Manduca sexta tissues. *J Insect Physiol* 52: 661–668, 2006.

Gingl E, French AS. Active signal conduction through the sensory dendrite of a spider mechanoreceptor neuron. *J Neurosci* 23: 6096–6101, 2003.

Gingl E, French AS, Panek I, Meisner S, Torkkeli PH. Dendritic excitability and localization of GABA-mediated inhibition in spider mechanoreceptor neurons. *Eur J Neurosci* 20: 59–65, 2004.

Hille C, Walz B. Dopamine-induced graded intracellular Ca^{2+} elevation via the Na^+Ca^{2+} exchanger operating in the Ca^{2+}-entry mode in cockroach salivary ducts. *Cell Calcium* 39: 305–311, 2006.

Hodgkin AL, Huxley AF. A quantitative description of membrane current and its application to conduction and excitation in nerve. *J Physiol* 116: 449–472, 1952.

Ianowski JP, O'Donnell MJ. Basolateral ion transport mechanisms during fluid secretion by Drosophila Malpighian tubules: Na^+ recycling, Na^+:K^+:$2Cl^-$ cotransport and Cl^- conductance. *J Exp Biol* 207: 2599–2609, 2004.

Jean-Xavier C, Mentis GZ, O'Donovan MJ, Cattaert D, Vinay L. Dual personality of GABA/glycine-mediated depolarizations in immature spinal cord. *Proc Natl Acad Sci USA* 104: 11477–11482, 2007.

Juusola M, Seyfarth E-A, French AS. Sodium-dependent receptor current in a new mechanoreceptor preparation. *J Neurophysiol* 72: 3026–3028, 1994.

Kaila K, Voipio J. GABA-activated bicarbonate conductance. Influence on EGABA and on postsynaptic pH regulation. In: *Chloride Channels and Carriers in Nerve, Muscle, and Glial Cells*, edited by Alvarez-Leefmans FJ, Russell JM. New York: Plenum Press, 1990, p. 331–352.

Kern R, van Hateren JH, Michaelis C, Lindemann JP, Egelhaaf M. Function of a fly motion-sensitive neuron matches eye movements during free flight. *PLoS Biol* 3: e171, 2005.

Lindemann JP, Kern R, van Hateren JH, Ritter H, Egelhaaf M. On the computations analyzing natural optic flow: quantitative model analysis of the blowfly motion vision pathway. *J Neurosci* 25: 6435–6448, 2005.

Loewenstein WR. Modulation of cutaneous mechanoreceptors by sympathetic stimulation. *J Physiol* 132: 40–60, 1956.

MacGregor RJ. *Neural and Brain Modeling*. San Diego, CA: Academic Press, 1987.

Marty A, Llano I. Excitatory effects of GABA in established brain networks. *Trends Neurosci* 28: 284–289, 2005.

Nusbaum MP, El Manira A, Gossard JP, Rossignol S. Presynaptic mechanism during rhythmic activity in vertebrates and invertebrates. In: *Neurons, Networks, and Motor Behavior*, edited by Stein PSG, Grillner S, Selverston AI, Stuart DG. Cambridge, MA: The MIT Press, 1997, p. 237–253.

Page AJ, Blackshaw LA. $GABA_B$ receptors inhibit mechanosensitivity of primary afferent endings. *J Neurosci* 19: 8597–8602, 1999.

Panek I, French AS, Seyfarth E-A, Sekizawa S-I, Torkkeli PH. Peripheral GABAergic inhibition of spider mechanosensory afferents. *Eur J Neurosci* 16: 96–104, 2002.

Panek I, Höger U, French AS, Torkkeli PH. Contributions of voltage- and Ca^{2+}-activated conductances to GABA induced depolarization in spider mechanosensory neurons. *J Neurophysiol* 99: 1596–1606, 2008.

Panek I, Torkkeli PH. Inhibitory glutamate receptors in spider peripheral mechanosensory neurons. *Eur J Neurosci* 22: 636–646, 2005.

Payne JA, Rivera C, Voipio J, Kaila K. Cation–chloride co-transporters in neuronal communication, development and trauma. *Trends Neurosci* 26: 199–206, 2003.

Rohrbough J, Spitzer NC. Regulation of intracellular Cl^- levels by Na^+-dependent Cl^- cotransport distinguishes depolarizing from hyperpolarizing

$GABA_A$ receptor-mediated responses in spinal neurons. *J Neurosci* 16: 82–91, 1996.

Rudomin P, Schmidt RF. Presynaptic inhibition in the vertebrate spinal cord revisited. *Exp Brain Res* 129: 1–37, 1999.

Sekizawa S-I, French AS, Höger U, Torkkeli PH. Voltage-activated potassium outward currents in two types of spider mechanoreceptor neurons. *J Neurophysiol* 81: 2937–2944, 1999.

Seyfarth E-A. Spider proprioception: receptors, reflexes, and control of locomotion. In: *Neurobiology of Arachnids*, edited by Barth FG. New York: Springer-Verlag, 1985, p. 230–248.

Seyfarth E-A, French AS. Intracellular characterization of identified sensory cells in a new spider mechanoreceptor preparation. *J Neurophysiol* 71: 1422–1427, 1994.

Shannon CE, Weaver W. *The Mathematical Theory of Communication*. Urbana, IL: Univ. of Illinois Press, 1949.

Sipilä ST, Schuchmann S, Voipio J, Yamada J, Kaila K. The cation–chloride cotransporter NKCC1 promotes sharp waves in the neonatal rat hippocampus. *J Physiol* 573: 765–773, 2006.

Sutor B, Grimm C, Polder HR. Voltage-clamp-controlled current-clamp recordings from neurons: an electrophysiological technique enabling the detection of fast potential changes at preset holding potentials. *Pflügers Arch* 446: 133–141, 2003.

Theander S, Edman A, Fahraeus C, Akoev GN, Grampp W. Cl^- transport in the lobster stretch receptor neurone. *Acta Physiol Scand* 167: 285–298, 1999.

Torkkeli PH, French AS. Simulation of different firing patterns in paired spider mechanoreceptor neurons: the role of Na^+ channel inactivation. *J Neurophysiol* 87: 1363–1368, 2002.

Torkkeli PH, Panek I. Neuromodulation of arthropod mechanosensory neurons. *Microsc Res Tech* 58: 299–311, 2002.

Widmer A, Höger U, Meisner S, French AS, Torkkeli PH. Spider peripheral mechanosensory neurons are directly innervated and modulated by octopaminergic efferents. *J Neurosci* 25: 1588–1598, 2005.

Zemkova HW, Bjelobaba I, Tomic M, Zemkova H, Stojilkovic SS. Molecular, pharmacological and functional properties of $GABA_A$ receptors in anterior pituitary cells. *J Physiol* 586: 3097–3111, 2008.